APPLIED ORGANOMETALLIC CHEMISTRY, VOL. 11, 163–179 (1997)

Low-Temperature Chemical Approaches for Synthesizing Sulfides and Nitrides of Reactive Transition Metals

M. A. Sriram, K. S. Weil and P. N. Kumta
Department of Materials Science and Engineering, Carnegie Mellon University, Pittsburgh, PA 15213, USA

The advent of the sol–gel technique over the past several decades and the recognition of its excellent flexibility for synthesizing a large variety of oxide ceramics and glasses in both bulk and thin-film forms has generated considerable interest in using solution-based processes to prepare ceramic materials. Because of the success of the sol–gel technique, a number of other chemical processes have been developed utilizing metalorganic/organometallic starting materials to create molecularly architectured precursors, which have proven effective in synthesizing both oxide and non-oxide materials. In the present study, two different chemical approaches have been implemented to synthesize non-oxides (sulfides and nitrides) of reactive transition-metal elements. Accordingly, a novel thio-sol–gel process for preparing TiS_2 and NbS_2 powders has been studied. In the case of TiS_2 synthesis, the chemical reaction has been examined in detail using Fourier-transform infrared spectroscopy (FTIR) and gas chromatography (GC). The effects of modification of the titanium precursor on the morphology of the final sulfide have also been investigated and are discussed. A second, more generalized process has been developed for synthesizing homogeneous precursors in multicomponent systems. Its utilization in preparing ternary nitrides has been demonstrated, and is also presented. © **1997 by John Wiley & Sons, Ltd.**

Keywords: sol–gel; ceramics; glasses; films; organometallic; titanium; niobium

1 INTRODUCTION

The traditional methods for synthesizing oxide and non-oxide ceramic powders typically involve reacting individual compounds or elements at high temperature for an extended period of time, and often require intermediate grinding steps to homogenize the material. Although the process culminates in the formation of crystalline powder, the prolonged duration of the reactions at high temperature results in highly agglomerated, large-grained particles. The intermediate grinding steps often introduce impurities which have deleterious influences on the properties of the ceramic. Furthermore, the low solid-state diffusion coefficients of the reacting species lead to compositional inhomogeneities in the final ceramic. Because of the need to tailor the electronic, optical, magnetic and mechanical properties in advanced ceramic components, which rely on careful control of the material's stoichiometry, microstructure and morphology, a number of alternative processing techniques have been developed.

The last few decades have witnessed considerable growth in the development and understanding of solution-based synthesis of ceramic precursors and powders. This is primarily because of several advantages offered by these processes, including synthesis of high-purity materials at low to moderate reaction temperatures, good molecular mixing in solution before heat treatment, and excellent control over the microstructure and morphology of the ceramic powder. Additionally, by controlling the molecular environment in solution it is possible to control the kinetics of the subsequent solution

CCC 0268–2605/97/020163–17

Received 10 January 1996
Accepted 12 May 1996

reactions to synthesize materials exhibiting different and unique morphology.

The sol–gel reaction involving the use of metal alkoxides is a classic example of the flexibility that solution synthesis offers in ceramics processing. Metal alkoxides are characterized by highly reactive alkoxy (—OR^-, R = alkyl) groups which make the metal atoms susceptible to nucleophilic attack.[1] These compounds have the ability to undergo hydrolysis in the presence of water, followed by polymerization due to condensation reactions which lead to the formation of the corresponding metal oxide. The hydrolysis and condensation reactions in solution can be controlled to a great extent by the use of an acid or a base catalyst, leading to either delayed or rapid condensation of the oxide molecular units resulting in the formation of a polymeric gel or a fine powder, respectively.[1] Depending on the extent of the two reactions the viscosity of the sol can be altered before complete gelation occurs, so that it can be spun to form thin and thick films, drawn to form fibers or cast to form bulk monoliths.[2] The gel can also be subjected to different drying conditions to yield either a low-density, high-surface-area aerogel or a more conventional, higher-density xerogel.[3] The difference in surface area between these two extremes can be significant, varying from $\sim 70\ m^2\ g^{-1}$ in the case of the xerogel up to $500\ m^2\ g^{-1}$ for an aerogel. Because of the flexibility demonstrated by the sol–gel process, it has become a very attractive method for fabricating a wide variety of oxide ceramics for use in electronic applications,[4, 5] particulrly those which require good ferroelectric[6] and dielectric properties.[7, 8] Similarly, the ability to synthesize high-purity, high-surface-area aerogels and powders has attracted considerable interest from researchers in the area of catalysis.[9]

A large body of literature has been published on the chemistry and application of the sol–gel technique for the synthesis of oxide, glass and glass ceramic fine particles as well as thin films. While the process is attractive for synthesizing oxide ceramics, its success has also provided an impetus for the development of other chemical processes based on the use of inorganic, organic and metalorganic/organometallic compounds as starting materials for building molecularly architectured ceramic precursors. Several reports have been published on the use of polymeric precursors to synthesize ceramics such as silicon carbide, silicon nitride and oxycarbide glasses and ceramics.[10–12] This strategy to synthesize a polymeric precursor so that carbon can be intentionally incorporated into the final ceramic involves the use of alkylmetal alkoxide precursors to synthesize silicon-oxycarbide glasses. The metal–alkyl and metal–alkoxy bonds in these precursors specifically provide the Si–C and Si–O linkages necessary to form the desired oxycarbide glass upon pyrolysis.

Our research in the chemical synthesis of ceramic materials is currently following two directions: (1) extension of the sol–gel process to synthesize non-oxide compounds and (2) development of a general technique which employs chelating agents to form multicomponent polymeric precursors to facilitate the synthesis of ternary nitride compounds. While there has been a concentrated effort to understand the precursor chemistry and the reaction mechanisms responsible for the oxide sol–gel process, there has not been much work conducted in extending this process for the synthesis of non-oxide ceramics. Melling and colleagues[13] have demonstrated the applicability of metal alkoxides for the synthesis of sulfides by reacting germanium alkoxide with H_2S. Since then, we have demonstrated the use of metal alkoxides to synthesize sulfides of reactive metals such as the rare earths.[14, 15] Apart from this work and several reports on synthesis of alkaline earth–rare earth sulfides,[16–18] there has not been much research directed towards utilizing the flexibility of the sol–gel process for the synthesis of non-oxides of reactive metals such as the early transition-metal elements.

Transition metal elements belonging to the Group IVB to VIB and their compounds are extremely oxophilic and tend to react vigorously with water or alcohols to form hydrated oxides or alkoxides. The use of non-hydroxylic solvents would therefore be necessary in studying the synthesis of non-oxide compounds of these elements from solution. Chianelli and Dines[19] have formed early transition-metal sulfides by reacting metal chlorides with inorganic sulfidizing agents such as NH_4HS and Li_2S in non-hydroxylic solvents. Schleich and co-workers[20] demonstrated the use of organic sulfidizing agents to initiate the sulfidization reaction with halide salts of some early transition metals. These two approaches have proven successful in synthesizing the sulfides directly at low temperatures, and in some cases even at room temperature. However, because of the rapid nucleation of the sulfide particles, fine particles

of either an amorphous or a poorly crystalline sulfide are formed. Control of defect structure, microstructure and morphology of the particles is extremely important for a number of applications which are sensitive to surface modifications and surface structure. It is of paramount importance, for example, in processing intercalation compounds such as TiS_2, a material which has potential application as a cathode in rechargeable lithium batteries.[21, 22] Alternative processing approaches which demonstrate a higher degree of control over the sulfide morphology are needed for this type of high-technology application. Section 2 of this paper discusses a thio-sol–gel process which has been used to synthesize TiS_2 and NbS_2. The technnique involves a reaction of metal alkoxides with H_2S to form a precursor which, when heat-treated in H_2S, yields the sulfide. The reaction mechanism in solution leading to the formation of these precursors has been studied, while also investigating the effect of the reaction and heat-treatment conditions on the evolution of the sulfide morphology.

The second strategy we have used to synthesize non-oxides involves the formation of a metalorganic hydroxide precursor which, when heat-treated in ammonia at moderate temperatures, yields the corresponding nitride. In particular, this approach has been used to prepare ternary transition-metal nitrides. Ternary nitrides are a relatively unexplored class of materials. They have been known to exhibit a number of important properties such as superconductivity,[23] catalytic activity,[24–27] thermal emissivity,[28] unusual magnetic behavior[29–32] and high hardness and strength[33–36] combined with good thermal and electrical conductivity. Until recently, however, much of the research has been focused on the synthesis and evaluation of the properties of binary nitrides, as higher-order nitrides are often much more difficult to prepare. The difficulty in their synthesis lies in the fact that nitrides in general tend to decompose at relatively low temperatures[37] (<1000 °C) because of the inertness and high bond energy of the N_2 molecule. This implies that the synthesis of ternary nitrides must be carried out at low temperatures. The low-reaction-temperature constraint usually means that the formation of ternary nitrides, if it occurs at all, requires very long reaction periods to allow enough time for the diffusion of the metal species in the solid state.

DiSalvo and co-workers have been successful in synthesizing a number of new ternary alkali and alkaline-earth metal nitrides, including the first layered ternary lithium nitride.[38–42] Their methodology exploits an inductive effect whereby the inclusion of electropositive elements such as the alkali metals tends to stabilize the ternary nitrides of transition or post-transition metals.[23, 43] Zur Loye and co-workers have taken an alternative synthesis approach, using transition-metal metallates as precursors to ternary transition-metal nitrides.[44] For example, hydrated mixed-metal molybdates are prepared by reacting an aqueous metal chloride, such as $FeCl_2$, with a solution of $Na_2MoO_4 \cdot (H_2O)_2$. The alkali salt that forms in this exchange reaction can be washed off and the hydrated mixed-metal molybdate can be dried and heat-treated in ammonia to form the ternary nitride.[45–47] Similarly, Herle *et al*. have synthesized layered $LiWN_2$ using the reaction of Li_2WO_4 with NH_3 at high temperatures.[48] Other synthesis strategies include nitridation of intermetallic compounds,[49–52] solid-state reaction between two metal compounds and ammonia or nitrogen[53, 54] and mechanical comminution of the binary nitrides followed by a high-temperature treatment in an atmosphere of ammonia or nitrogen.[55]

Most of the above approaches require either prolonged heat treatments or a combination of long soaking times at high temperatures. However, as discussed earlier, such high-temperature reactions inevitably lead to problems of decomposition, agglomeration, impurity contamination and compositional inhomogeneity, which are deleterious to the electrical, mechanical and magnetic properties of the final nitride. The excellent molecular mixing attainable in the polymer precursor approach offers the opportunity to generate precursors that have clusters or molecular structural units representative of the ultimate desired compound. The formation of these units at low temperatures leads to reduction in the diffusion distances that the components need to travel in order to form the desired phase. Thus, materials which normally form at high temperature and require long soaking times can be synthesized with enhanced kinetics at low to moderate heat-treatment temperatures. In Section 3 of this paper we present a complex-precursor approach which leads to the facile synthesis of ternary nitride compounds and shows promise in preparing and identifying new ternary and higher-order transition-metal nitrides. The two techniques discussed in this paper offer the

possibility of synthesizing non-oxide compounds in a wide range of powder morphologies and material forms, including thin films. Additionally, the processes also offer the exciting prospects of preparing new ceramic materials for a number of electronic, magnetic and structural applications.

2 THIO-SOL–GEL PROCESS FOR THE SYNTHESIS OF TiS_2 AND NbS_2

2.1 Experimental procedure

2.1.1 Synthesis of TiS_2

Two different reaction routes were implemented for synthesizing TiS_2. In all the experiments, titanium isopropoxide was used as-received from Johnson Matthey, technical-grade H_2S was obtained from Matheson gases, and benzene was used after distilling over sodium chips and molecular sieves. Benzenesulfonic acid was used as-received from Aldrich. All manipulations during the reaction as well as handling of the precursors were accomplished in the absence of air.

Reaction 1

$Ti(OPr^i)_4$ was dissolved in benzene, and H_2S gas was bubbled through it at room temperature. A black precipitate was observed within 1 min, but the bubbling was continued for 10 min to ensure completion of the reaction.

Reaction 2

After dissolution of $Ti(OPr^i)_4$ in anhydrous benzene, benzenesulfonic acid (BSA, from Aldrich) was added in a molar ratio of 10:1 (alkoxide/acid) in order to modify the alkoxide. The mixture was stirred to dissolve the acid and H_2S gas was bubbled through it for 10 min. A black precipitate was seen to form within 2 min.

In both cases, the reaction vessel was sealed and isolated for 12 h before the precipitate was collected. Each precipitate was collected in a Soxhlet extractor and washed thoroughly with benzene. The filtrate from the reactions appeared dark brown in color. The powders from both the reactions were further dried for 3 h in a vacuum oven at 40 °C and were perceived to be very air-sensitive. Elemental chemical analyses on all the powders were conducted by Galbraith Laboratories Inc. (Knoxville, TN, USA). They were also heat-treated in flowing H_2S at 600, 700 and 800 °C for a period of 6 h. X-ray diffractograms (θ/θ diffractometer, Rigaku, Tokyo, Japan) were collected on the as-prepared precipitates and the heat-treated powders. All the powders were also observed under an SEM (Series 4, CamScan, Cambridge, UK) to study and compare the evolution of their morphology. Samples for SEM examination were prepared by ultrasonicating the powders in hexane for 5 min and placing a few drops of the suspension on a graphite stub.

The first reaction was studied in greater detail to elucidate the molecular reactions occurring in solution. An infrared (IR) spectrum was obtained from the powder in a KBr pellet using a Fourier-transform infrared (FTIR) spectrometer (113V; Brucker Instruments, Billerica, MA, USA, with a mercury cadmium telluride detector), in the 4000–600 cm^{-1} wavenumber range. The transmission spectrum in the range 500–200 cm^{-1} was collected using a CsI pellet in a Biorad FTIR spectrometer equipped with a DTGS detector and CsI optics. The dark brown filtrate was distilled and gas chromatography (GC) (5830A; Hewlett Packard, Avondale, PA, USA) was performed on the distillate to identify the products of the reaction. After ensuring that all the excess benzene was distilled off, chemical analysis was performed on the dark brown liquid. The liquid was also analyzed employing electron impact mass spectroscopy (Model 7070; VG Analytical, Manchester, UK).

2.1.2 Synthesis of NbS_2

The synthesis of a precursor for NbS_2 was carried out along the lines of reaction 2 detailed above, using acetonitrile as a solvent. Niobium ethoxide [$Nb(OEt)_5$] was dissolved in dry acetonitrile and BSA was added to it in a ratio of 1:10 (BSA/alkoxide). When H_2S was passed through the solution, the reaction proceeded similarly to reactions 1 and 2 described in Section 2.1.1. The reaction product was filtered to obtain a black precipitate and a clear, dark filtrate. The filtrate could not be thoroughly washed since the fine nature of the powder caused the filter paper to clog. The powder collected after filtration was dried as before under vacuum for 3 h at 40 °C. The dried powder was heat-treated in flowing H_2S for 6 h at 700 °C and 800 °C respectively. XRD patterns were collected on the heat-treated powders.

2.2 Results and discussion

2.2.1 Synthesis of TiS_2

2.2.1.1 Synthesis of precursors

The reaction of titanium alkoxide with hydrogen sulfide generated both solid and liquid products. Since the sulfidization reaction in solution has hardly been studied, an attempt was made to investigate Reaction 1 in greater detail. Accordingly, both the liquid and solid products of the reaction were analyzed using various analytical techniques. Chemical analysis of the as-precipitated powder from the first reaction (dried at 40 °C) showed an S/Ti molar ratio of about 1.4:1 and an O/Ti molar ratio of 1.2:1 (see Table 1). The IR spectra collected for the precipitate from 2000 to 900 cm^{-1}, shown in Fig. 1, and from 500 to 200 cm^{-1} (see the inset in Fig. 1) and indicate the existence of isopropoxy groups. The doublet seen at 1377 and 1360 cm^{-1} is representative of the characteristic *gem*-dimethyl structure of the isopropoxy group.[56, 57] In addition, absorptions characteristic of isopropoxy groups bonded to titanium are observed at 1160, 1127 and 1013 cm^{-1},[57] while the Ti–S vibrations can be seen centered around 300 cm^{-1}.[19] The IR and chemical analysis results indicate that the reaction in solution leads to the incorporation of sulfur by a possible replacement of the alkoxy groups attached to the titanium center.

In order to understand the replacement reaction instrumental for the incorporation of sulfur, the liquid was distilled and analyzed using GC,

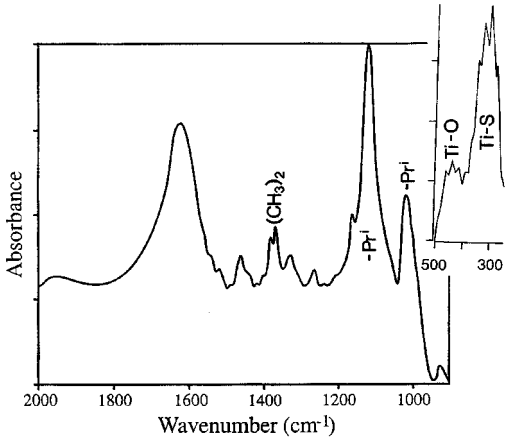

Figure 1 Infrared spectrum collected for the precipitate obtained from reaction 1 (titanium isopropoxide with H_2S) showing absorptions characteristic of Ti—OPr^i and Ti—S bonds (inset).

which showed that isopropanol was liberated during the reaction. This, in combination with the IR results, therefore suggests a replacement of the isopropoxy (—OC_3H_7) groups by thiol (—SH) groups from H_2S, resulting in the liberation of isopropanol from the alkoxide. However, the replacement is not complete, as indicated by the presence of isopropoxy groups in the solid formed due to the reaction. The attack of the alkoxy groups by the thiol species would form the basis of a thiolysis reaction (Scheme 1) very similar to the hydrolysis reactions seen in the sol–gel process

$$H_2S + Ti(OR)_4 \rightarrow H_2S \rightarrow Ti(OR)_4 \rightarrow (HS)(OR)_3Ti\leftarrow \underset{\displaystyle R}{\overset{\displaystyle |}{OH}} \rightarrow Ti(OR)_3SH + ROH$$

Scheme 1

The overall sulfidization reaction can therefore be written as Eqn [1].

$$Ti(OR)_4 + nH_2S \underset{n\leq 4}{\longrightarrow} Ti(OR)_{4-n}(SH)_n + nROH \quad [1]$$

From the above, it can be seen that the thiolysis reaction of titanium isopropoxide leads to the formation of alkoxy–thiol species. The formation of the black precipitate is indicative of further condensation–polymerization of the alkoxy–thiol species by the liberation of H_2S, represented by Eqn [2].

$$2p\{Ti(OR)_{4-n}(SH)_n\} \overset{n\leq 4}{\rightarrow} \{(RO)_{4-n}(SH)_{n-1}Ti— S—Ti(SH)_{n-1}(OR)_{4-n}\}_p + p\,H_2S \quad [2]$$

p is variable and $R = C_3H_7$

The condensation reaction [2] has been verified by estimating the isopropanol liberated using quantitative GC and correlating it with calculated amounts derived from the chemical analyses of the solid precipitate and the liquid product.[58, 59] The formation of an azeotrope in the benzene–isopropanol system greatly simplified the quantitative analysis of the liquid products of the reaction. The results indicated the extent to which the thiolysis reaction [1] had occurred, and also indicated that all the thiol groups condensed to form Ti–S–Ti linkages in the solid according to Eqn [2] (i.e. partial thiolysis and complete condensation of the thiol groups).

Chemical analysis conducted on the liquid product showed an S/Ti molar ratio of about 0.07 : 1. In addition, the mass fragmentation pattern of the liquid was identical to that of titanium isopropoxide, implying that the dark liquid was in fact the alkoxide, which had not undergone significant reaction with H_2S. Some of the alkoxide molecules remained unreacted, possibly due to (a) association in inert solvents such as benzene (titanium isopropoxide is known to have an average molecular complexity of 1.4 in benzene[60]), or (b) due to the formation of partially reacted soluble oligomers which do not undergo any further reaction in benzene because of steric hindrance to nucleophilic attack by H_2S. Experiments conducted in acetonitrile (a coordinating solvent which is known to offer a better medium for the dissociation of H_2S) have shown more than a five-fold increment in product yield, providing support to the hypothesis.

The above results suggest that competition between thiolysis and condensation reactions plays an important role in controlling the amount of sulfur incorporated into the precursor. Accordingly, significant variation in the structure of the precursors could be envisaged by effecting changes in the thiolysis and condensation reactions. This could be achieved in a number of ways, e.g. by changing or modifying the reactants, using different solvent systems, etc. Thus reaction 2 was conducted and the precipitate was chemically analyzed; the results are shown in Table 1. The precursors derived from the two reactions contain similar amounts of sulfur (in terms of the molar ratio of sulfur to titanium). The sulfur and oxygen contents reflect the extent of reaction of the alkoxy groups on Ti, the presence of oxygen being due to alkoxy groups that have not been replaced (as shown in the IR spectrum of the precipitate in reaction 1). The carbon contents (reflecting residual hydrocarbons) are higher in powders obtained from reaction 2 in comparison with reaction 1. This is probably because of modification with a bulky benzenesulfonyl group in reaction 2. These variations reflect the different molecular processes responsible for the formation of precursors leading to different molecular structures. These structural changes in the precursors could have an impact on the temperature of formation of TiS_2, the crystallite size and the evolved morphology of the sulfide.

Table 1 Chemical analysis of precursors obtained from reactions 1 and 2

	Analysis (wt%)					
Reaction	Ti	S	C	H	O[a]	S/Ti[b]
1	33.6	32.3	17.3	3.5	13.3	1.4
2	32.3	30.3	20.8	3.5	13.1	1.4

[a] Oxygen obtained from balance.
[b] Molar ratio of sulfur to titanium in the precursor.

2.2.1.2 Conversion of precursors to crystalline sulfides

All the precipitated precursors were amorphous and the X-ray diffraction patterns collected for the heat-treated powders obtained from the two reactions are shown in Figs 2(a) and (b). In both the processes adopted, crystalline TiS_2 (hexagonal phase) was seen to form after heat treatment at 600 °C for 6 h in an H_2S environment. The powder obtained from reaction 2 shows broader peaks, indicating smaller crystallite sizes. How-

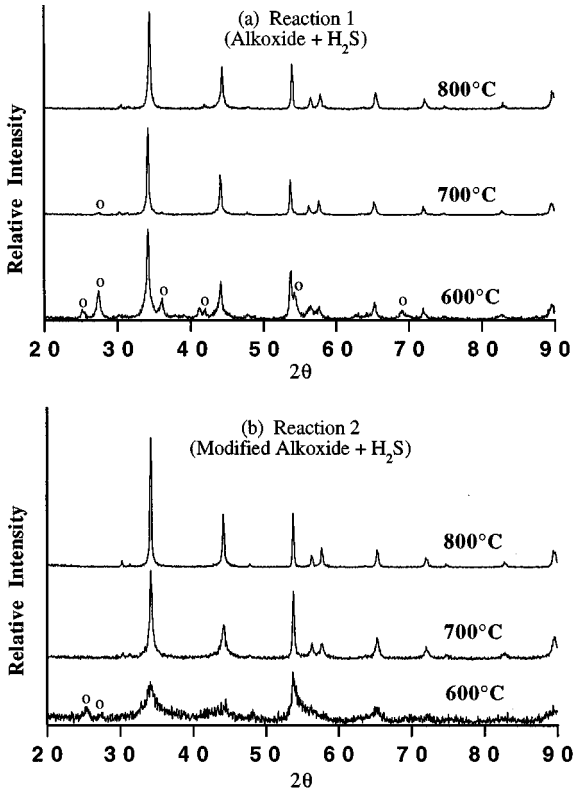

Figure 2 X-ray diffraction patterns (using Cu K_α radiation) collected for samples obtained from (a) reaction 1 and (b) reaction 2, heat-treated for 6 h in flowing H_2S at 600 °C, 700 °C and 800 °C. The 'O' marks indicate the positions of oxygen peaks. All other peaks are due to hexagonal TiS_2.

ever, crystalline TiO_2 phases (both rutile and anatase) are also formed at this temperature in both the reactions due to the unreplaced alkoxy groups that condense to form Ti—O—Ti bonds as represented by Eqn [3].

$$Ti—OR + RO—Ti \rightarrow Ti—O—Ti + \text{hydrocarbons} \quad [3]$$

When heat-treated at 700 °C, the XRD pattern obtained for the powder from reaction 2 indicates single-phase TiS_2, while for the powder from reaction 1, an oxide peak with a low relative intensity is still visible. The formation of a single phase at 700 °C is probably due to either the fine crystallite size or the presence of more carbon in this precursor (as shown in Table 1), which could accelerate the conversion to TiS_2. However, we have observed that single-phase TiS_2 could be synthesized using the precursor obtained from reaction 1 when it is subjected to a 10 h heat treatment at 700 °C. Upon heat treatment at 800 °C in flowing H_2S, both precursors transform to TiS_2 in 6 h. In addition, control experiments conducted by heat-treating sol–gel-derived TiO_2 in flowing H_2S at 800 °C under identical conditions showed TiO_2 as the major phase in the XRD pattern. This implies that the kinetics of the sulfidization reaction at high temperature of the thio-sol–gel derived precursors are enhanced due to the incorporation of sulfur at the precursor stage.

Differences evidenced in the XRD patterns could be due to variations in the molecular structure of the precursors. This is also reflected in the unique morphologies observed in the as-prepared precursors and the sulfide formed upon heat treatment of these precursors.

2.2.1.3 Morphologies of the precursors and the crystalline sulfide

The morphologies of the as-precipitated and heat-treated powders obtained from both reactions are shown in Figs 3 and 4. As can be seen, the precipitates in Figs 3(a) and 4(a) are composed of spherical particles. It should also be

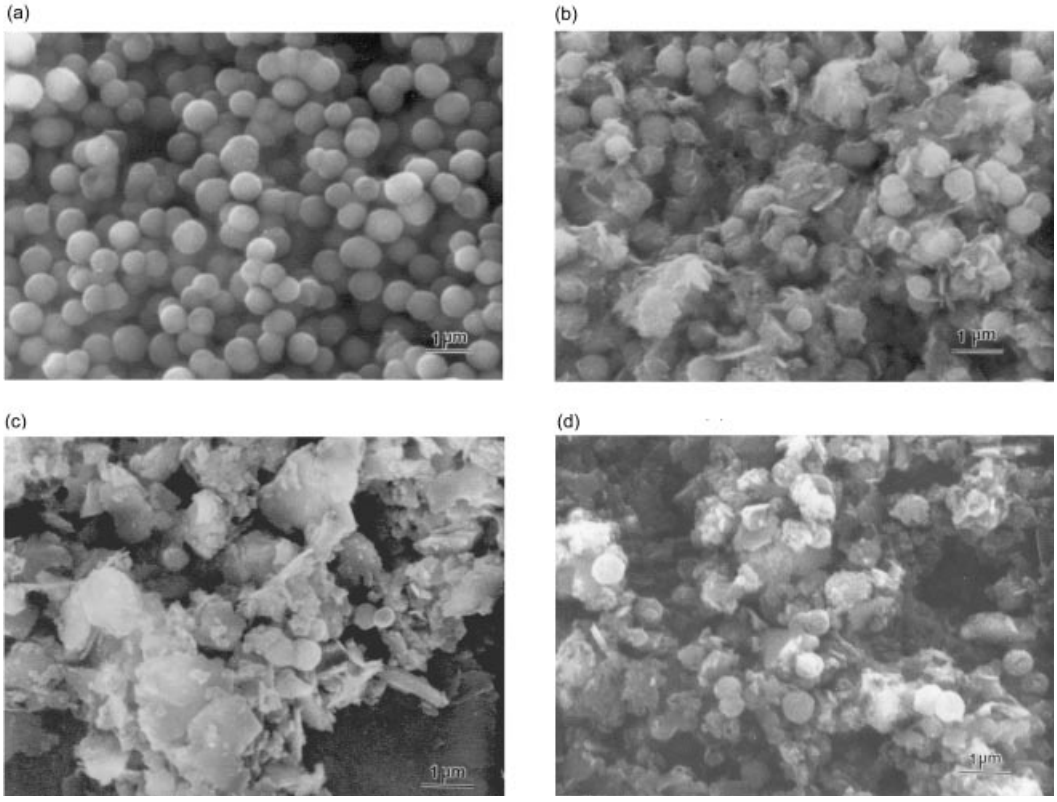

Figure 3 SEM micrographs of precipitate obtained from the reaction of titanium isopropoxide with H_2S (a), and heat-treated for 6 h in flowing H_2S at 600 °C (b), 700 °C (c), and 800 °C (d). The formation of TiS_2 platelets causes a distinct change in the morphology.

noted that the monodispersed particle size distribution of the precipitates obtained using reaction 1, seen in Fig. 3(a), points to the fact that the rate of thiolysis is much slower than the rate of condensation.[61] This helps to maintain the concentration of the condensable species (Eqn [1]) below the critical concentration necessary for homogeneous nucleation. As a result, condensation of any new species generated occurs on the particles already formed during the initial burst of nucleation, leading only to growth.

The particles from reaction 1 are about 0.5 μm in diameter, while those from reaction 2, shown in Fig. 4(a), are about 2 μm in diameter. The variations in particle size and distribution in the two reactions reflect differences in the sulfidization rates, leading to the formation of condensable species (Eqn [1]) and their subsequent condensation to form the precipitate (Eqn [2]). Such an explanation would warrant a detailed study of the mechanisms involved in the formation of the precursors for the second reaction similar to that done for the first reaction.

The SEM micrographs of the sulfide powders obtained by heat treatment of the precursors at 600, 700, and 800 °C in flowing H_2S display interesting differences in morphology, as shown in Figs 3(b)–(d) and 4(b)–(d). The precursors from reaction 1 show the formation of platelets of TiS_2 at 600 °C (see Fig. 3b) which are separated from the spherical precursor particles. At 700 and 800 °C (see Figs 3(c) and (d)) there are very few spherical particles, and sintered agglomerates of smaller platelets and spheres and large platelets are visible. In comparison, the particles obtained after heat treatment of the precursors from reaction 2 show retention of the overall spherical morphology seen at the precursor stage. At 600 °C, as shown in Fig. 4(b), it is clear that the TiS_2 platelets have grown from these spheres with their *c*-axes normal to the radial direction of the transformed sphere. Although the platelets grow in size, this overall

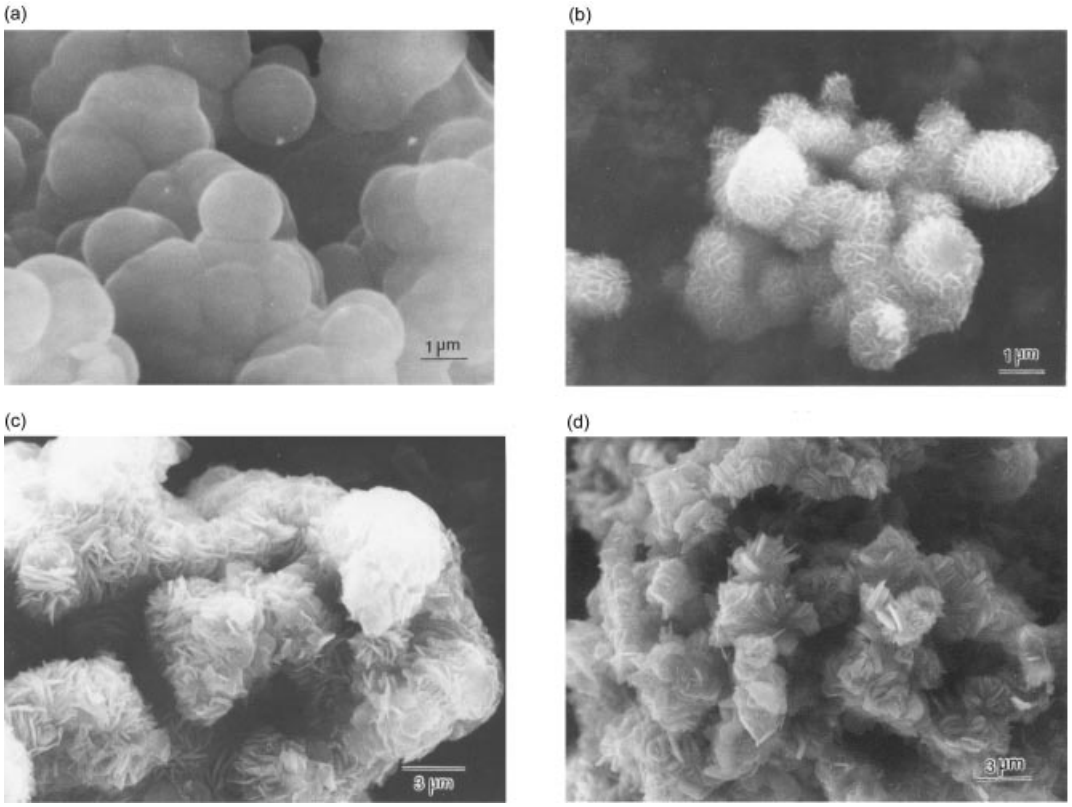

Figure 4 SEM micrographs of precipitate obtained from the reaction of modified titanium isopropoxide with H_2S (a) and heat-treated for 6 h in flowing H_2S at 600 °C (b), 700 °C (c) and 800 °C (d). TiS_2 platelets grow from the spheres while maintaining the overall spherical morphology of the precipitate.

morphology is maintained at 700 and 800 °C as shown in Figs 4(c) and (d). The origin of these variations is still unknown; however, based on the observations and information from the literature, some possible mechanisms could be proposed.

The XRD results indicate that crystalline TiS_2 as well as crystalline TiO_2 form during the course of the reaction. Formation of TiS_2 involves a contribution of sulfur (a) from the precursor and (b) from the reaction of unreplaced alkoxy groups with H_2S, as well as (c) from the reaction of Ti—O—Ti bonds (in the form of TiO_2 as well as in an amorphous phase) with H_2S. It therefore appears that the observed morphological differences are due to a combination of (a) differences in molecular structure of the precursor and (b) the rate of transformation of the amorphous alkoxy–sulfide to the crystalline sulfide.

The coordinating groups on titanium could influence the condensation of the unreplaced alkoxy groups to form Ti—O—Ti bonds, and therefore the crystallization of TiO_2. In the case of reaction 2, a large fraction of the alkoxy groups could have reacted with H_2S at a relatively low temperature before they condensed to form Ti—O—Ti bonds, while in reaction 1 condensation of alkoxy groups could have occurred early, thus leading to differences in observed amounts of crystalline TiO_2. The reaction of these oxide groups with H_2S to form Ti—S—Ti bonds causes the release of H_2O. The rate of release of water is essentially dependent on the rate of the sulfidization reaction. Water released could influence the morphology, as has been observed in the case of the synthesis of MoS_2 thin films[62, 63] (MoS_2 has a layered structure similar to TiS_2). Thus, differences in the molecular structure could have an important influence not only on the amount of crystalline TiO_2, but also on the sulfidization reaction. Hence the relevant aspects of molecular structure that are being investigated for this purpose are the titanium molar density of the precursor and the average coordination environment of the titanium atoms (which together will represent the structure of the network).

This study demonstrates the flexibility of the thio-sol–gel process to synthesize TiS_2 with unique morphologies. This control of morphology in the case of TiS_2 is probably only seen in this approach among all the hitherto existing chemical techniques. This variation and control is achievable only because of the partial thiolysis reaction in the precursor development stage, as discussed above. In this sense, the inability of H_2S to replace the alkoxy groups completely is compensated for by the control of morphology and crystallite size that is possible. This control is not only obtained by modifying the alkoxide as explained above, but also by using various sulfidizing agents to generate the intermediate precursors.[59] These different morphologies could exhibit very different surface characteristics affecting the properties of the material, for example the kinetics of the lithium intercalation reaction in the case of TiS_2. Consequently, it can be expected that these morphologies could significantly impact the electrochemical performance of TiS_2 as a cathode material. Results of electrochemical studies of thio-sol–gel-synthesized TiS_2, that have been published elsewhere,[64] do indicate a significant influence of the morphology and microstructrure on the electrochemical utilization of TiS_2 cathodes in rechargeable lithium batteries.

2.2.2 Synthesis of NbS_2

Preliminary XRD results (Fig. 5) clearly show the feasibility of the thio-sol–gel process for the synthesis of NbS_2. The broad diffracted peaks obtained for the powder heat-treated at 700 °C for 6 h in flowing H_2S indicate the formation of fine particles of single-phase hexagonal NbS_2; the pattern is also devoid of any peaks of niobium oxides. At 800 °C the peaks are sharper and have all been indexed to hexagonal NbS_2. This shows that metal alkoxides are indeed viable precursors for the synthesis of early transition-metal sulfides. The reaction mechanism has not been studied in detail but is

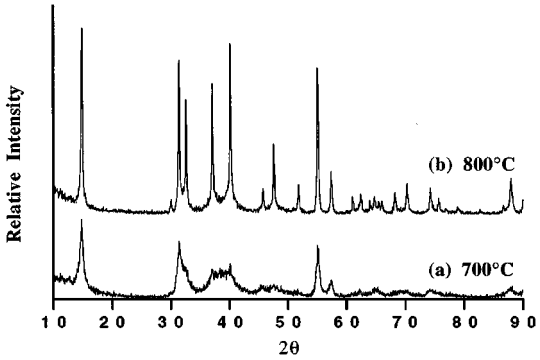

Figure 5 Precursor obtained by the reaction of $Nb(OEt)_5$ with H_2S heat-treated at 700 °C (a) and at 800 °C (b) in flowing H_2S for 6 h, showing single-phase hexagonal NbS_2.

expected to be similar to that observed in the case of titanium. The fact that the powder is black could indicate the formation of Nb—S bonds in the precursor through a thiolysis–condensation mechanism causing the release of ethanol. A more detailed study is currently in progress to pinpoint the extent of this reaction and to evaluate the influence of the reaction in solution as well as the effect of the gas–solid reaction (during heat treatment) on the evolved morphology of NbS_2.

3 COMPLEXED PRECURSOR APPROACH FOR THE SYNTHESIS OF TERNARY NITRIDES

3.1 Experimental procedure

The procedure developed for synthesizing ternary transition metal nitrides is comprised of essentially three sequential reaction steps: (1) the formation of a polymeric liquid precursor; (2) the hydrolysis of this precursor to form a metal-organic hydroxide; and (3) the pyrolysis and ammono-
lysis of the hydroxide precursor to yield the ternary nitride.

3.1.1 Materials and equipment

All inorganic metal chlorides were used as received: $AlCl_3$ (99.99%; Aldrich), $FeCl_2 \cdot 4H_2O$ (99.995%; Fisher Scientific), $MoCl_5$ (99.9%; Aldrich), $NiCl_2 \cdot 6H_2O$ (99.9999%; Aldrich), $TiCl_4$ (99.9%; Aldrich), and WCl_6 (99%; Aldrich). HPLC-grade acetonitrile (Fisher Scientific) and ethanolamine (99%; Sigma) were used without further purification. The water used for the hydrolysis reaction was doubly distilled and de-ionized to a resistivity of 18.3 MΩ cm or greater. Electronic-grade ammonia (Mattheson Gas) was used for the pyrolysis and ammonolysis of the mixed-metal precursors. All chemical manipulations were conducted in an argon atmosphere glovebox (O_2 and $H_2O \leqslant 5$ ppm) or under a protective stream of UHP nitrogen unless otherwise noted. All glassware used was acid-washed with NoChromix and oven dried before use.

3.1.2 Reaction 1: formation of the liquid precursor

Three ternary systems were investigated in this study: Ni–Mo–N, Fe–W–N and Ti–Al–N. The liquid precursors were prepared using the following procedure. In the glovebox, the corresponding metal chlorides were measured in stoichiometric molar ratios, typically using 4–10 g samples, and loaded along with a Teflon-coated magnetic stir bar and approximately 100 ml of acetonitrile into a 500 ml three-necked round-bottom flask. After the flask had been appropriately sealed, it was transferred to a fume hood and connected to the UHP nitrogen line. Once the chlorides were thoroughly dissolved, ethanolamine was added to the solution through a septum using a syringe and needle. The measured amount of ethanolamine added was determined assuming complete replacement of the chloride by ethanolamine, and depended on the quantity and nature of the metal chloride used. Since the chelation reaction of ethanolamine is in general exothermic and some hydrogen chloride gas is evolved, the ethanolamine was added at slow rate of approximately 2 ml min^{-1}. In all cases the chelation reactions occurred nearly instantaneously, as evidenced by color changes in the acetonitrile solution and by the formation of a syrupy colored liquid separate from the acetonitrile phase. When the addition of ethanolamine was complete, the flask was shaken for several minutes to ensure complete mixing. Eventually a two-phase mixture formed which separated into a thick, colored polymeric liquid that settled to the bottom of the flask while a clear acetonitrile phase remained on the top.

3.1.3 Reaction 2: precipitation of the metalorganic hydroxide

Once the polymeric liquid precursor was prepared, the flask was opened and approximately 100 ml of water was added to the parent liquor with vigorous stirring. In some cases, depending on the metal system, hydrolysis occurred quickly, forming a precipitate within several minutes. In other cases the chelated liquid simply dissolved in the cold water. The entire liquor was heated to distil off the acetonitrile, and refluxed for approximately 4 h at 95–100 °C to force the hydrolysis reaction to completion. The resultant precipitate was vacuum-filtered and washed with five bed-volumes of water. In each case, the effluent did not appear to include any metal-containing species, as evidenced by its clear color.

3.1.4 Reaction 3: pyrolysis and ammonolysis

Upon filtration, the precipitate was dried overnight under vacuum at 80 °C, after which it was

removed from the filter paper and lightly crushed with an agate mortar and pestle. A sample of the precursor was weighed in a high-purity alumina boat, which was placed in a 2.5 in (6.35 cm) diameter quartz flow-through tube furnace. The back end of the tube furnace was connected to a bubbler and the front end was connected to the gas line. Before the heat treatment was initiated, the tube was purged for 10 min with commercially pure nitrogen, then purged for another 5 min with ammonia gas. All samples were fired in slow-flowing (0.5–1 l min^{-1}) ammonia under the same conditions: ramp from room temperature to 120 °C at 10 °C min^{-1} and hold at 120 °C for 1 h; followed by a ramp from 120 °C to 950 °C at 3 °C min^{-1} and hold at 950 °C for 4 h; and finally the samples were allowed to furnace-cool. The powders were reweighed after pyrolysis and analyzed for their crystalline phases and microstructure.

3.1.5 Materials characterization

The precursors and heat-treated powders were analyzed by X-ray diffraction (XRD). Powder samples were mounted on glass slides and analyzed using a Rigaku (Theta–Theta) diffractometer. In all cases, graphite-filtered Cu Kα radiation was used. The data for each compound was collected using a scan rate of 1.5° min^{-1} and a step size of 0.05°. SEM characterization was conducted using an AMRAY 1810 microscope equipped with a Robinson backscatter detector. The ratios of metals in the nitrides were determined by energy-dispersive X-ray analysis using an EDAX DX-4 analyzer.

3.2 Results and discussion

3.2.1 Synthesis of the liquid mixed-metal precursor (reaction 1)

The precursors are generated by reaction of the metal chlorides with ethanolamine. It is well known that the transition-metal chlorides behave as Lewis acids and tend to form adducts with electron-donating bases such as hydrazine and alkylamines.[65] The presence of two strong nucleophilic centers (OH^- and NH_2^-) on ethanolamine make it a strong bidentate ligand with good chelating properties. In view of this, it is suspected that the transition-metal chlorides react neat with ethanolamine by replacing one or more chlorine species from the metal chloride and releasing HCl to form a chelated product. This reaction could be written in the case of molybdenum chloride, for example, as in Eqn [4].

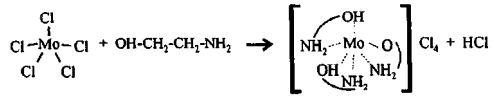

(1) [4]

Similar reactions have been reported for the complexes of ethanolamine and chromium, nickel or cobalt halides.[66–68] The extent of replacement will depend upon the amount of HCl released. Product (**1**), written as molybdenum ethoxyamine chloride, can react further with ethanolamine to form a diethoxyamine chloride. However, the extent of subsequent reactions will depend on the kinetics of the replacement reaction, which in part depend upon steric and electrostatic interactions between the attached and unattached ethanolamine groups. The high viscosity of the liquid precursor does indicate its polymeric nature. Product (**1**) could therefore further react, either with ethanolamine to replace a second chloride, as in (**2**), or with a second $MoCl_5$ or metalorganic unit to form an oligomer (**3**). Detailed analysis of the molecular processes in solution will need to be conducted to verify the exact mechanism involved in the formation of the polymer. We have carried out the neat reaction between $MoCl_5$ and ethanolamine and have shown that it yields hydrogen chloride gas and a very thick, sticky, red–brown liquid as products. When heat-treated in ammonia at 650 °C this liquid precursor yields γ-Mo_2N.

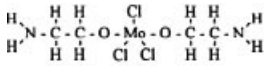

(**2**)

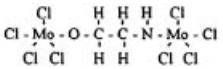

(**3**)

In acetonitrile, it is expected that the transition-metal chlorides form complexes which are soluble. For example, in the case of $MoCl_5$, it is known that acetonitrile forms an end-on and a side-on coordinated adduct, depending on the way in which Mo is linked to the polar nitrile species of CH_3CN.[69] End-on adducts could be replaced by weak bases such as hydrazine.[70] Thus, it is possible that ethanolamine could replace the adduct of $MoCl_5$ formed in acetonitrile and yield products very similar to those envisaged above.

With the exception of $TiCl_4$ and $AlCl_3$, all of

the metal chlorides dissolved readily in acetonitrile; $TiCl_4$ and $AlCl_3$ are known to form solid adducts with acetonitrile. These adducts eventually dissolve in excess acetonitrile with vigorous stirring. After dissolving the three sets of metal chlorides (Ni–Mo, Fe–W and Ti–Al) in acetonitrile, ethanolamine was added to each solution. In each case the reaction occurred immediately, with each ethanolamine droplet resulting in two products: (1) a colored, sticky, liquid droplet, which eventually settled to the bottom of the flask or smeared along the inside wall of the vessel, and (2) a cloudy, white material which eventually seemed to dissolve in the acetonitrile. For the first 10–20 drops of ethanolamine, hydrogen chloride gas formed in the space above the acetonitrile solution. Even after the gas evidently cleared from inside the flask, white fumes of a low-pH gas continued to evolve from the bubbler for several minutes afterwards.

Color changes in these reactions are indicative of the rate of complexation with ethanolamine. Since all of the precursors are dark in color, it is difficult to ascertain exactly the change in their color as the ethanolamine is added. However, the color of the acetonitrile solution was readily apparent, and its change with the addition of ethanolamine demonstrates that the precursor does not initially form stoichiometrically with respect to the final desired metal ratio. For example, the nickel–molybdenum chloride–acetonitrile solution changes from lime green to bright neon green to chocolate brown to colorless as ethanolamine is added. Thus it is probable that the metal chlorides display preferential affinity towards ethanolamine, resulting in the formation of numerous complexed product compositions up to the final addition of ethanolamine. Assuming that the various metal and mixed-metal ethanolamine complexes are soluble in each other, the final liquor should be a stoichiometric mixture.

3.2.2 Precipitation of the mixed-metal metalorganic hydroxide (reaction 2)

The liquid precursors obtained from the reactions between the metal chlorides and the ethanolamine, conducted in acetonitrile, are soluble in excess ethanolamine and water. Except for the Ti–Al–N precursor, in which hydrolysis occurs rapidly, the precursors are quite stable in air and require prolonged exposure to water before precipitation occurs. In the case of the Ti–Al–N precursor, a precipitate formed within 5 min after the addition of cold water. The other two precursors required refluxing to force the hydrolysis reaction. After filtration and drying, each of the precursors was distinctive in color. In general, the morphologies of these powders are relatively featureless, appearing as fine 1–10 μm agglomerates after grinding, as indicated by the SEM micrographs shown in Figs 6(a), (b) and (c). In two of the three cases, Ni–Mo–N and Fe–W–N, the agglomerates comprise spherical particles that are in the submicrometer size range. In these two compounds hydrolysis proceeds slowly, giving rise to homogeneous nucleation of the metalorganic hydroxide which leads to the formation of spherical precipitate particles. The morphology of the hydrolyzed Ti–Al–N precursor, on the other hand, contains very few homogeneously nucleated spherical particles and primarily comprises large agglomerates of irregularly shaped prticles; this reflects the rapid rate of the hydrolysis reaction.

These precursor powders were also subjected to XRD analysis. The data shown in Figs 7(a)–(c) indicate that two of the dried precursors are amorphous, while the Fe–W–N precursor is crystalline. This compound has been indexed to the orthorhombic crystallographic system; however, the diffraction pattern does not match any of the obvious simple or mixed-metal oxides or hydroxides listed in the PDF database. While it is difficult at this point to speculate on the mechanism by which the liquid precursors are hydrolyzed, it is expected that the precipitate is a metalorganic hydroxide, possibly of the type (**4**) or (**5**). The hydroxides could have formed by the replacement of the NH_2 groups in (**2**) with hydroxyl groups to form (**4**) or by the replacement of the M—Cl (M = metal) bonds with M—OH to form the chelated hydroxide (**5**). The variations **4** and **5** may be viewed as extremes in a spectrum of the possible metalorganic hydroxide structures which may form. The extent to which each hydroxide resembles one or the other structure type is dictated by the electropositive, oxophilic nature of the metal cations involved and the conditions under which the hydrolysis reaction occurs.

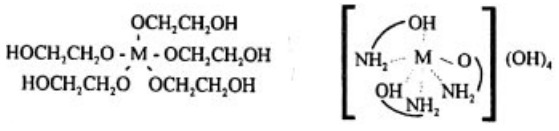

(**4**) (**5**)

3.2.3 Conversion of the hydroxide precursor to a crystalline nitride (reaction 3)

The hydrolyzed powders convert to yield the corresponding single-phase ternary nitrides upon heat treatment in ammonia at 950 °C in 4 h. The rapid rate of formation of the nitride at moderate temperature suggests that the hydrolysis reaction leads to the formation of a complexed mixed-metal hydroxide rather than complexed individual-metal hydroxides. However, it is also known that the presence of hydrocarbons during ammonolysis significantly accelerates the formation of nitrides, particularly in the case of AlN.[71] Detailed gas evolution studies will be essential to determine the nitridation mechanism.

The XRD traces obtained for the powders heat-treated in ammonia are shown in Figs 8(a) and (b) for the Ni–Mo–N and Fe–W–N powders, respectively. Each pattern is phase-pure and nearly identical to that reported in the literature for the respective nitrides, Ni_3Mo_3N and $FeWN_2$.[22, 23] The XRD powder pattern collected for the nitrided powder belonging to the Ti–Al–N system, shown in Fig. 8(c), was not representative of a highly crystalline material. However, the peaks did correspond to the reported PDF pattern for Ti_3AlN.[72] The ratios of metal contents in each nitride were confirmed

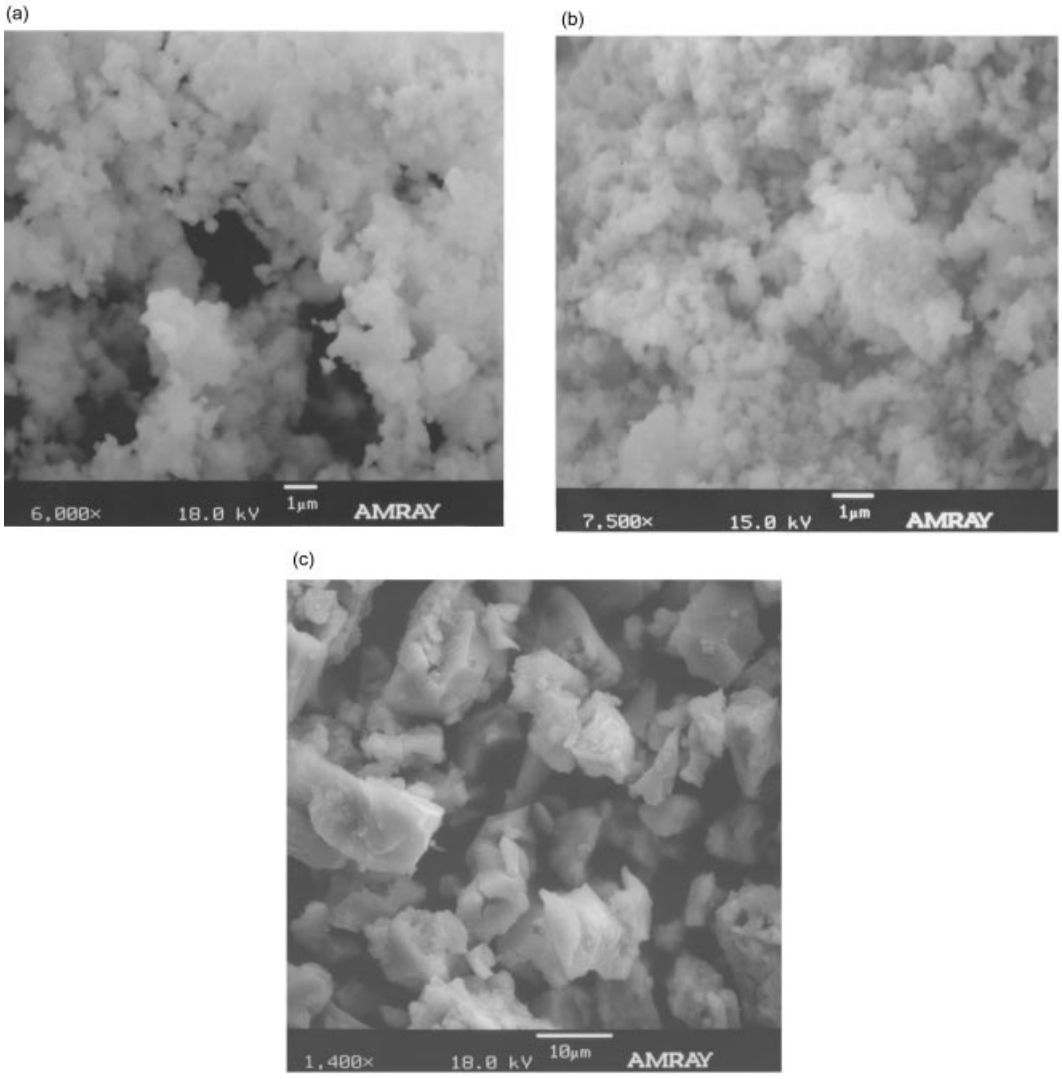

Figure 6 SEM micrographs showing the morphology of the dried precursors in the following ternary systems: (a) Ni–Mo–N, (b) Fe–W–N and (c) Ti–Al–N.

qualitatively using EDAX and are given in Table 2.

The morphologies of the ternary nitride powders were observed by SEM and are shown in Figs 9(a), (b) and (c). In all cases, the heat treatment causes significant changes in the microstructure of the initial precursor powders. For example, in the case of Ni_3Mo_3N it can be seen that, upon reacting with ammonia, the initially spherical particles present in the precursor have experienced a morphological change, resulting in the formation of cuboidal particles less than 0.5 μm in size. Under the conditions of heat treatment employed, these particles have further sustained considerable

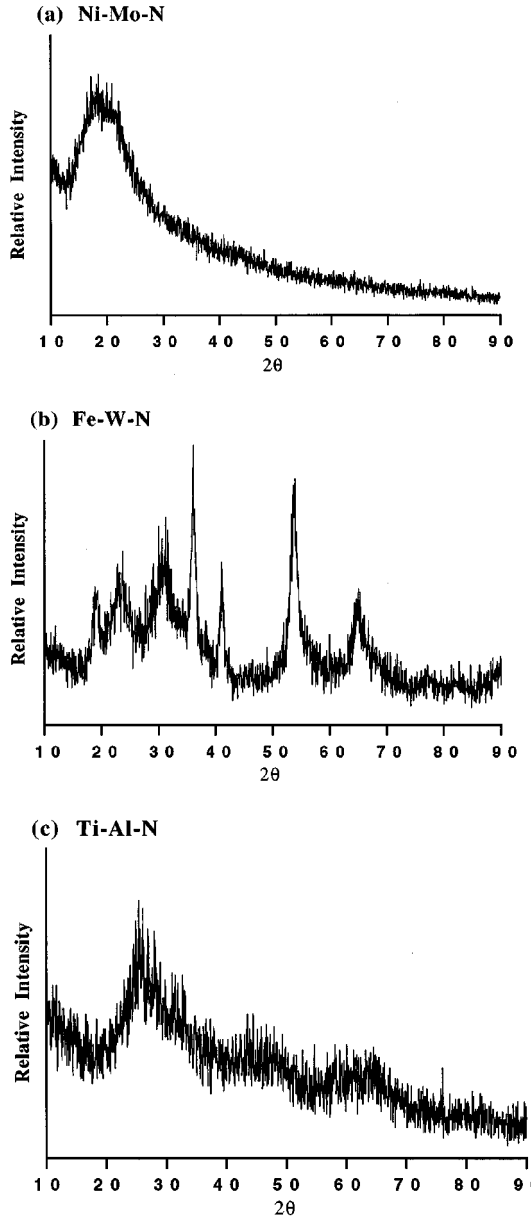

Figure 7 X-ray diffraction patterns for the following hydrolyzed and precipitated ternary powders: (a) Ni–Mo–N, (b) Fe–W–N and (c) Ti–Al–N.

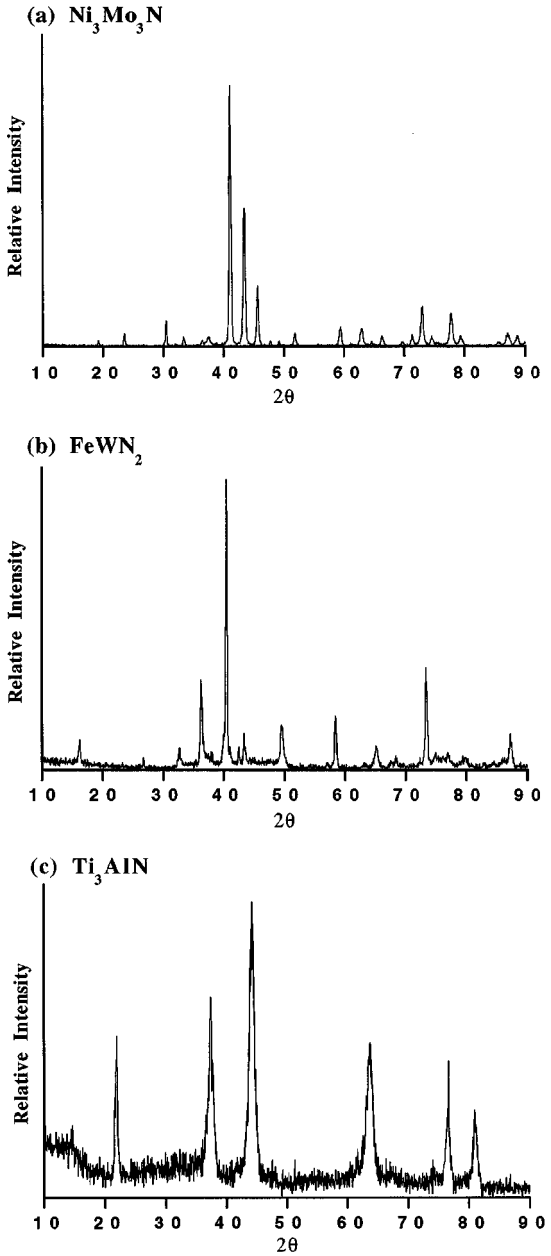

Figure 8 X-ray diffraction patterns for the following ternary powders, heat-treated at 950 °C for 4 h in ammonia: (a) Ni_3Mo_3N, (b) $FeWN_2$ and (c) Ti_3AlN.

Table 2 Energy-dispersive X-ray chemical analysis of nitride powders

Material A–B–N	A (at %)/B (at %)
Ni–Mo–N	0.96
Fe–W–N	0.95
Ti–Al–N	3.19

necking to form agglomerates several micrometers in size, as shown in Fig. 9(a).

Similarly, from Fig. 9(b) it can be seen that in the case of $FeWN_2$ the precursor, which comprises irregularly shaped agglomerates of spherical particles, has transformed to a very fine (< 0.5 μm) crystalline powder. Again, the nitride particles have undergone significant necking due to the prolonged treatment at 950 °C, resulting in the formation of agglomerates several micrometers in size. Likewise, a similar agglomerated state is seen, though to a much higher degree, in the as-heat-treated Ti_3AlN powders (see Fig. 9c). The aggregation and necking of the fine-scale particles observed in each nitride powder indicate that the ammonia heat treatment requires optimization. It is believed that the heat treat-

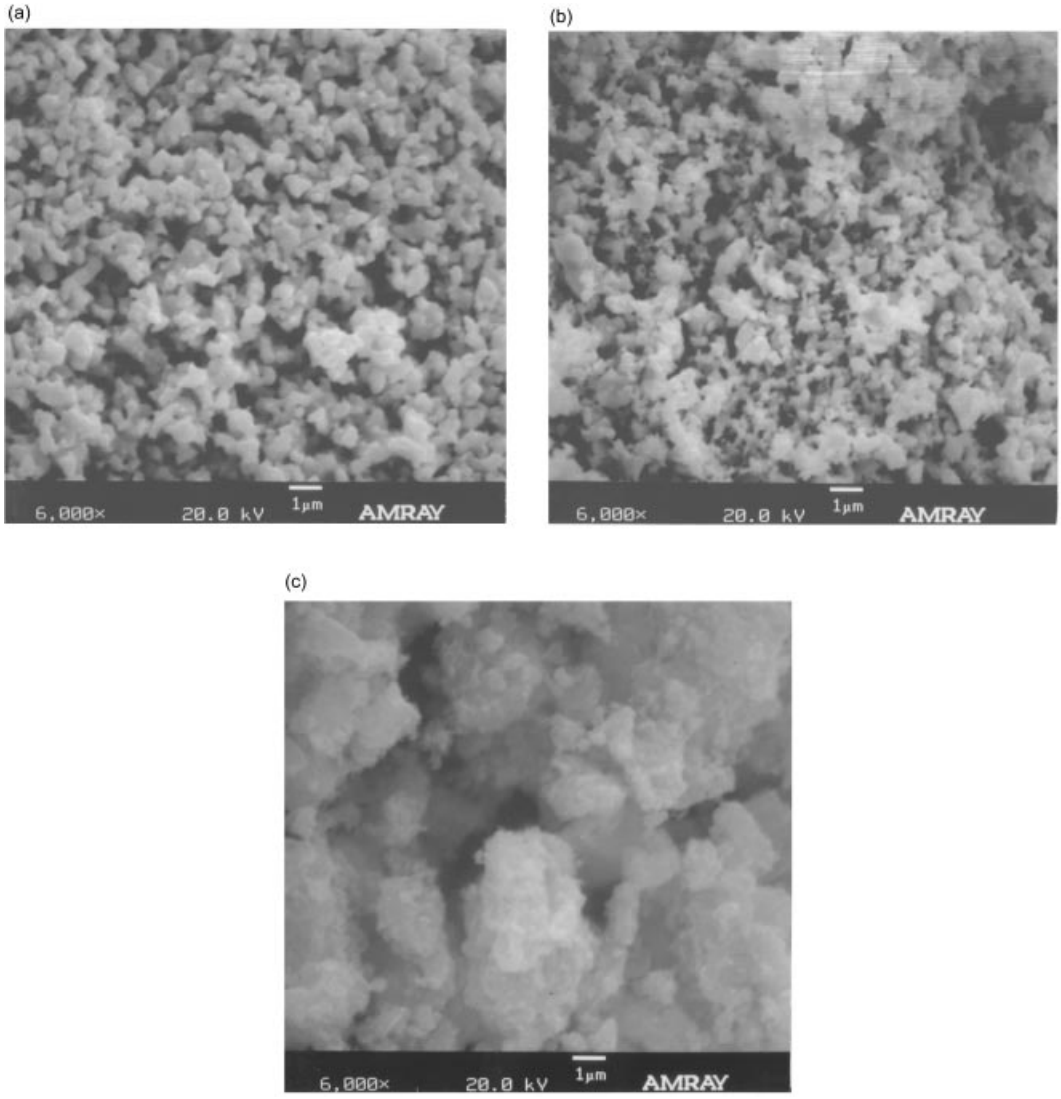

Figure 9 SEM micrographs showing the morphology of the nitride powders obtained after heat-treating the precursors at 950 °C for 4 h in ammonia: (a) Ni_3Mo_3N, (b) $FeWN_2$ and (c) Ti_3AlN.

ment could be optimized with respect to temperature and time to prevent or minimize the formation of these sintered agglomerates and to yield fine (<0.5 μm) ternary nitride powders.

4 SUMMARY

The early transition metals tend to be oxophilic, making it difficult to synthesize single-phase non-oxide ceramic powders from these elements. The two metalorganic-based techniques described in this paper offer the potential not only to control carefully the stoichiometry of binary and higher-order transition-metal sulfides and nitrides, but they also offer the opportunity to control the morphology of the non-oxide powder. The thio-sol–gel process, used so far to synthesize TiS_2 and NbS_2 powders, consists of the formation of an alkoxy–sulfide precursor through a thiolysis–condensation mechanism. When heat-treated in H_2S, the precursor yields the sulfide at temperatures as low as 600 °C. The composition and structure of the precursor appear to play an important role in the kinetics of transformation to the sulfide phase. The combined influence of these factors is also seen in the morphology of the resultant crystalline TiS_2 powder that is evolved upon heat treatment. The use of a modifying agent helps to change the sulfidization reaction in solution, which in turn affects the transformations of the precursor to TiS_2 powder. The powder thus formed exhibits vastly different morphologies. In a similar manner, $Nb(OC_2H_5)_5$ has been reacted with H_2S to form a precursor which transforms to hexagonal NbS_2 at 700 °C.

The synthesis of ternary nitrides, often difficult because of the instability of nitrides at the temperatures necessary for solid-state diffusion of the constituent elements, has been shown to be tractable by using a chelated metalorganic hydroxide precursor. Reactions between ethanolamine and metal chlorides dissolved in acetonitrile yield viscous, polymeric liquids which are relatively stable in air. These liquid precursors can be hydrolyzed by adding a relatively large volume of water and refluxing the resulting solution for several hours at 95–100 °C. The precipitate which forms can be filtered, dried and heat-treated in ammonia to form a ternary nitride. Three such nitrides which have been prepared using this technique have been identified by XRD and SEM analyses to be Ni_3Mo_3N, $FeWN_2$ and Ti_3AlN. The thio-sol–gel and complexed precursor approaches, both demonstrate the flexibility of metalorganic-based processes in synthesizing bulk and thin-film forms of non-oxide ceramic materials. The approaches also offer considerable promise for the preparation of these non-oxide materials with control of stoichiometry and microstructure which are useful for a number of electronic, magnetic and structural applications.

Acknowledgements The authors acknowledge the support of the US National Science Foundation (Grants DMR 9301014 and CTS 9309073 and ARPA (Contract No. 14-94-1-0773) for funding the work. One of the authors (KSW) also acknowledges the support of the US Department of Defense.

REFERENCES

1. J. Livage, M. Henry and C. Sanchez, *Prog. Sol. State Chem.* **18**, 259 (1988).
2. C. J. Brinker and G. W. Scherer, *Sol–Gel Science*, *The Physics and Chemistry of Sol–Gel Processing*, Academic Press, Boston, 1990, pp. 841–864.
3. Ref. 2, pp. 518–526.
4. D. R. Ulrich, *J. Non-Cryst. Sol.* **100**, 174 (1988).
5. D. R. Ulrich, *J. Non-Cryst. Sol.* **121**, 465 (1990).
6. P. P. Phule, T. A. Deis and D. G. Dindiger, *J. Mater. Res.* **6**, 1567 (1991).
7. J. F. MacDowell and G. H. Beall, in: *Materials and Processes for Microelectronic Systems*. Proc. 1st Int. Science and Technology Conf., Nair, K. M., Pohanka, R. and Buchman, R. C. (eds), *Ceram. Trans.* **V15**, American Ceramic Society, Ohio, 1989, p. 259.
8. (a) R. Hsu, P. N. Kumta and T. P. Feist, *J. Mater. Sci.* **30**, 3123 (1995); (b) J. Y. Kim, R. Hsu and P. N. Kumta, *J. Am. Ceram. Soc.* **79**(6), 1473 (1996).
9. V. L. S. Teixeira da Silva, E. I. Ko, M. Schmal and S. T. Oyama, *Chem. Mater.* **7**, 179 (1995).
10. H. Zhang and C. G. Pantano, *J. Am. Ceram. Soc.* **73**, 958 (1990).
11. G. M. Renlund, S. Prochazka and R. H. Doremus, *J. Mater. Res.* **6**, 2716 (1991).
12. K. Kuroda, Y. Tanaka, Y. Sugahara and C. Kato, *Better Ceramics Through Chemistry III*, *Proc. Spring Meeting Mater. Res. Soc.* **121**, 575 (1988).
13. P. J. Melling, *Ceram. Bull.* **63**, 1427 (1984).
14. P. N. Kumta and S. H. Risbud, *Prog. Cryst. Growth Charact.* **22**, 245 (1991).
15. P. N. Kumta and S. H. Risbud, *Mater. Sci. Eng.* **B18**, 260 (1993).
16. Y. Han and M. Akinc, *J. Am. Ceram. Soc.* **74** (1), 2815 (1991).

17. L.-H. Wang, M.-H. Hon and W.-L. Huang, *Mater. Res. Bull.* **26**, 649 (1991).
18. M.-S. Tsai, L.-H. Wang and M.-H. Hon, *J. Am. Ceram. Soc.* **78** (5), 1185 (1995).
19. R. R. Chianelli and M. B. Dines, *Inorg. Chem.* **17**, 2758 (1978).
20. A. Bensalem and D. M. Schleich, *Mater. Res. Bull.* **23**, 857 (1988).
21. M. S. Whittingham and J. A. Panella, *Mater. Res. Bull.* **16**, 37 (1981).
22. P. G. Bruce and M. Y. Saidi, *J. Sol. State Chem.* **88**, 411 (1990).
23. F. J. DiSalvo, *Science* **247**, 649 (1990).
24. L. Volpe and M. Boudart, *J. Sol. State Chem.* **59**, 332 (1985).
26. R. B. Levy and M. Boudart, *Science* **181**, 547 (1973).
27. L. Volpe and M. Boudart, *Catal. Rev.-Sci. Eng.* **27**, 515 (1985).
28. A. J. Perry, M. Georgson and W. D. Sproul, *Thin Solid Films* **157**, 255 (1988).
29. K. H. J. Buschow, R. Coehoorn, D. B. De Mooij, K. de Waard and T. H. Jacobs, *J. Magn. Magn. Mater.* **92**, L35 (1990).
30. Y. Otani, D. P. F. Hurley, H. Sun and J. M. D. Coey, *J. Appl. Phys.* **69**, 5584 (1991).
31. S. Miraglia, J. L. Soubeyroux, C. Kolbeck, O. Ishard, D. Fruchart and M. Guillot, *J. Less Commun. Met.* **171**, 51 (1991).
32. K. H. J. Buschow, *J. Magn. Magn. Mater.* **100**, 79 (1991).
33. T. S. Oyama, *J. Sol. State Chem.* **96**, 442 (1992).
34. L. E. Toth, *Transition Metal Carbides and Nitrides*, Academic Press, New York, 1971.
35. H. Randhawa, P. C. Johnson and R. Cunningham, *J. Vac. Sci. Technol.* **A6**, 216 (1988).
36. U. Konig, *Surf. Coat. Technol.* **33**, 91 (1987).
37. F. J. DiSalvo, *Science* **247**, 649 (1990).
38. P. E. Rauch and F. J. DiSalvo, *J. Sol. State Chem.* **100**, 160 (1992).
39. M. Y. Chern and F. J. DiSalvo, *J. Sol. State Chem.* **88**, 459 (1990).
40. M. Y. Chern and F. J. DiSalvo, *J. Sol. State Chem.* **88**, 528 (1990).
41. D. A. Vennos, M. E. Badding and F. J. DiSalvo, *Inorg. Chem.* **29**, 4059 (1990).
42. S. H. Elder, L. H. Doerrer and F. J. DiSalvo, *Chem. Mater.* **4**, 928 (1992).
43. M. Y. Chen, D. A. Vennos and F. J. DiSalvo, *J. Sol. State Chem.* **96**, 415 (1992).
44. J. D. Houmes, D. S. Bem and H.-C. zur Loye, in: *Covalent Ceramics II*: *Non-oxides*, Barron, A. R., Fischman, G. S., Fury, M. A. and Hepp, A. F. (eds), *Proc. Mater. Res. Soc.* **V327**, 153 (1993).
45. D. A. Bem, J. D. Houmes and H.-C. zur Loye, in: *Covalent Ceramics II*: *Non-Oxides*, Barron, A. R., Fischman, G. S., Fury, M. A. and Hepp, A. F. (eds), *Proc. Mater. Res. Soc.* **V327**, 165 (1993).
46. D. S. Bem, C. P. Gibson and H.-C. zur Loye, *Chem. Mater.* **5**, 397 (1993).
47. D. S. Bem and H.-C. zur Loye, *J. Sol. State Chem.* **104**, 467 (1993).
48. P. S. Herle, M. S. Hegde, N. Y. Vasanthacharya, J. Gopalakrishnan and G. N. Subbanna, *J. Sol. State Chem.* **112**, 208 (1994).
49. A. Gudat, R. Kniep and A. Rabenau, *Thermochim. Acta* **160**, 49 (1990).
50. A. Gudat, R. Kniep, A. Rabenau, W. Bronger and U. Ruschewitz, *J. Less Common Met.* **159**, L29 (1990).
51. T. Brokamp and H. Jacobs, *J. Alloys Compounds* **176**, 47 (1991).
52. H. Jacobs and E. von Pinkowski, *J. Less Common Met.* **146**, 147 (1989).
53. P. Hohn, S. Haag, W. Milius and R. Kniep, *Angew. Chem.* **103**, 374 (1991).
54. W. A. Groen, M. J. Kraan and G. de With, *J. Mater. Sci.* **29**, 3161 (1994).
55. W. A. Groen, M. J. Kraan, G. de With and M. P. A. Viegers, in: *Covalent Ceramics II*: *Non-oxides*, Barron, A. R., Fischman, G. S., Fury, M. A. and Hepp, A. F. (eds), *Proc. Mater. Res. Soc.* **V327**, 239 (1993).
56. J. V. Bell, J. Heisler, H. Tannenbaum and J. Goldenson, *Anal. Chem.* **25**, 1720 (1953).
57. C. T. Lynch, K. S. Mazdiyasni, J. S. Smith and W. J. Crawford, *Anal. Chem.* **36**, 2332 (1964).
58. M. A. Sriram and P. N. Kumta, *J. Am. Ceram. Soc.* **77** (5), 1381 (1994).
59. M. A. Sriram and P. N. Kumta, *Mater. Sci. Eng.* **B33**, 140 (1995).
60. D. C. Bradley, R. C. Mehrotra and W. Wardlaw, *J. Chem. Soc.* 5020 (1952).
61. E. A. Barringer and H. K. Bowen, *Langmuir* **1**, 414 (1985).
62. V. Buck, *Thin Solid Films* **139**, 157 (1986).
63. P. D. Fleischauer, *Thin Solid Films* **154**, 309 (1987).
64. M. A. Sriram, P. N. Kumta and G. E. Blomgren, in 'Role of Ceramics in Advanced Electrochemical Systems', Proceedings of the 97th Annual Meeting of the American Ceramic Society, Cincinnati, Ohio, 30 April to 3 May, 1995, Kumta, P. N., Rohrer, G. S. and Balachandran, U. (eds); *Ceramic Transactions* **65**, (163) (1996).
65. F. A. Cotton and G. Wilkinson, *Advanced Inorganic Chemistry*, John Wiley, New York, 1988, p. 792.
66. V. V. Udovenko and O. N. Stepaneko, *Russ. J. Inorg. Chem.* **14**, 91 (1969).
67. V. V. Udovenko and Y. S. Duchinskii, *Russ. J. Inorg. Chem.* **12**, 510 (1967).
68. V. V. Udovenko and A. N. Gerasenkova, *Russ. J. Inorg. Chem.* **12**, 654 (1967).
69. M. A. Sriram, P. N. Kumta, J. P. Matoney and E. I. Ko, *J. Mater. Sci. Lett.* **14**, 906 (1995).
70. M. A. Sriram, P. N. Kumta and E. I. Ko, *Chem. Mater.* **7**, 859 (1995).
71. S. Colque and P. Grance, *J. Mater. Sci. Lett.* **13**, 621 (1994).
72. Powder Diffraction File no. 37-1140.